ELSEVIER

Contents lists available at ScienceDirect

# Computational Materials Science

journal homepage: www.elsevier.com/locate/commatsci



# Density functional theory analysis of the effect of structural configurations on the stability of GaAsBi compounds



Husain Adamji<sup>a</sup>, Margaret Stevens<sup>b</sup>, Kevin Grossklaus<sup>b</sup>, Thomas E. Vandervelde<sup>b</sup>, Prashant Deshlahra<sup>a,\*</sup>

- <sup>a</sup> Department of Chemical and Biological Engineering, Tufts University, Medford, MA 02155, USA
- <sup>b</sup> Department of Electrical and Computer Engineering, Tufts University, Medford, MA 02155, USA

#### ABSTRACT

The aggregation of Bi atoms exhibits significant influence on the stability and electronic properties of GaAsBi compounds. Here, density functional theory calculations are used to probe stabilities of different configurations of Bi atoms substituted for As at concentrations below 4% of available As sites. The configurations examined include ensembles of four or eight Bi atoms with large Bi-Bi distances (dispersed configuration) or Bi atoms occupying contiguous As sites (aggregated configurations) in periodic supercells of different sizes. The stabilities of GaAsBi compounds decrease with increasing Bi concentration. This decrease in stability is more significant for dispersed than aggregated configurations, which leads to increased favorability for the aggregation of Bi atoms at higher concentration. Among the aggregated arrangements, the linear and planar ones are much more stable than the three-dimensional arrangements at all concentrations. The stabilities also depend significantly on ensemble sizes of Bi atoms, with enhanced stability for linear [1 0 1] and planar (1 1 1) configurations in eight atom ensembles than in four atom ensembles of similar concentration. These results demonstrate distinct effects of concentration and ensemble size on the preferred configuration and suggest that accurate large-scale simulations of doped GaAs compounds require models that incorporate not only atom-pair interactions but also long-range interactions among aggregates.

#### 1. Introduction

The last five decades have witnessed rapid growth in processing power of electronic devices driven by decreasing sizes and increasing densities of transistors. With silicon-based transistors approaching their size and speed limits, the focus on III-V compound semiconductors has increased greatly due to their wide range of structures and electronic properties [1]. GaAs based compounds, in particular, have had significant technological impacts due to their direct band-gaps, high electron mobility and operability over wide temperature ranges. GaAs can also form ternary or quaternary compounds with other elements in Group-III (e.g., Al, In) and Group-V (e.g., P, Sb, Bi) of the periodic table, which imparts remarkable tunability to the band gaps of these materials [2,3].

GaAsBi ternary compounds have been studied with great interest because Bi incorporation lowers the band gap of GaAs without significant loss of electron mobility for dilute concentrations [3–6]. Such materials are reported to have decreased bandgap temperature sensitivity and exhibit suppressed Auger recombination [7,8]. However, the Bi atoms are much larger than the As atoms they replace in the ternary compound, which induces significant local strain in the lattice. The clustering of Bi atoms to decrease lattice strain tends to deteriorate

electron mobility and photoluminescence [2]. X-ray absorption spectra (XAFS) and transmission electron micrographs have shown that increasing Bi concentrations lead to changes in prevalent Bi atom configurations from atom pairs to extended planar ordering analogous to CuPt crystals prior to phase separation of Bi into clusters [9–11].

Density functional theory (DFT) studies show a decrease in band gap with Bi incorporation into GaAs, as observed in experiments, and have found strong spin-orbit coupling in GaAsBi, which leads to significant asymmetry between electron and hole mobility [12,13]. These calculations involved ordered configurations of uniformly separated Bi atoms and did not probe the relative stabilities of different Bi configurations at the low Bi concentrations that allow stable GaAsBi compounds without droplet formation. More detailed studies on Bi-terminated GaAs (001) surfaces combined DFT with cluster expansion and Monte Carlo simulations to determine thermodynamically stable surface configurations of Bi and analyze surface reconstructions observed in STM studies [14,15]. Recent aberration corrected annular dark-field imaging studies and DFT analysis for linear and dispersed Bi configurations in GaAsBi films grown by metalorganic vapor phase epitaxy has shown that Bi atoms prefer to form linear arrangements in [100] and [110] directions instead of random distributions [16].

Here, we use DFT to probe stabilities of Bi atom configurations in

E-mail address: prashant.deshlahra@tufts.edu (P. Deshlahra).

<sup>\*</sup> Corresponding author.

bulk GaAsBi systems with partial substitution of As by Bi at various values below 4% of the total As sites to assess the influence of Bi concentration on ordering preferences. These studies confirm some clustering preferences proposed from experiments [9,16,17] and provide more detailed information that may be utilized for developing cluster expansion models for larger systems and identifying opportunities for the engineering of more stable Bi based materials.

#### 2. Methods

Periodic density functional theory (DFT) calculations were performed within the Vienna ab initio Simulation Package (VASP 5.4.4) [18,19] using the Perdew-Burke-Ernzerhof (PBE) [20] version of the exchange correlation functional, which is based on the generalized gradient approximation (GGA). Dispersion corrections were not applied to the GGA energies, but some comparisons with DFT-D2 correction of Grimme [21] were made for relative energies of different types of Bi configurations, as shown in Supporting Information (Table S1). The wave functions of valence electrons were described using plane-wave basis functions included up to a kinetic energy cutoff of 400 eV. The interactions between atoms cores and valence electrons were treated using the projector augmented wave method [22]. Electronic structures were converged self-consistently to energy differences less than  $1 \times 10^{-5}$  eV between successive iterative steps. Geometries were optimized until forces on atoms were below 0.01 eV Å $^{-1}$ .

The non-spin-polarized energies of 8-atom primary unit cells of GaAs with zinc blende structure were calculated using a  $4\times4\times4$  Monkhorst-Pack k-points mesh [23,24] with lattice constants varied in steps of 1% around the experimental value (5.654 Å [25]). The change in energy as a function of lattice constant was fit to a quadratic equation to determine the minimum energy. The DFT lattice constant with minimum energy was 5.778 Å, which is 2.2% larger than the experimental value. Such slight over prediction of lattice constants is typical of GGA functionals, which tend to delocalize electron densities slightly more than is expected for densities of real wavefunctions [26]. Analogous relaxation for an isomorphous GaBi unit cell led to 6.477 Å lattice constant, which is 2.3% larger than the predicted lattice constant (6.33 Å [5,27]) for this compound.

GaAsBi compounds were modeled using periodic supercells containing  $5 \times 5 \times 5$ ,  $4 \times 4 \times 4$  and  $3 \times 3 \times 3$  zinc blende unit cells with 500, 256, and 108 Ga atoms, respectively, and equal numbers of group V atoms, as shown in Fig. 1. Four or eight As atoms in these supercells were substituted with Bi, which led to Bi concentrations between 0.8 and 3.7% of the total group V atoms, as shown in Table 1. Based on the calculated GaAs and GaBi lattice constants and Vegard's law, such low Bi concentrations would lead to lattice expansions below 0.45% of pure

**Table 1**GaAsBi supercell sizes and Bi concentrations.

Supercell	Number of atoms			Bi concentration (% of group V sites)	
	Ga	As	Bi	_	
$3 \times 3 \times 3$	108	104	4	3.7	
$4 \times 4 \times 4$	256	252	4	1.6	
$4 \times 4 \times 4$	256	248	8	3.1	
$5 \times 5 \times 5$	500	496	4	0.8	
$5 \times 5 \times 5$	500	492	8	1.6	

GaAs. Energies of some GaAsBi configurations containing 3.7% Bi were calculated using the lattice constant stretched to values derived from Vegard's law for this concentration [28]. The absolute values of these energies were lower than those obtained for the same configuration using the lattice constant of pure GaAs by less than 2 kJ mol<sup>-1</sup> (details in Supporting Information, Table S2). However, the relative energies of the configurations remain within 0.1 kJ mol<sup>-1</sup> of each other for the stretched and unstretched system. Therefore, these small expansions were considered negligible for relative stability of different configurations at same Bi concentrations and all calculations were performed using the DFT-derived minimum energy lattice constant of pure GaAs. The absolute stabilities for these calculations are underestimated by ~1.9 kJ mol<sup>-1</sup> for 3.7% Bi, and by smaller values for lower Bi concentrations. The 3  $\times$  3  $\times$  3, 4  $\times$  4  $\times$  4 and 5  $\times$  5  $\times$  5 supercells consisted of cubes of edge lengths 17.34 Å, 23.11 Å and 28.89 Å, respectively. The first Brillouin zone for these large-supercell calculations was sampled only at the Gamma-point. These calculations were performed without spin-polarization. Calculated energies for some structures were compared to spin-polarized calculations and were found to have essentially identical energies.

Energies of gas-phase As and Bi atoms were determined using spin-polarized calculations of isolated atoms at the center of a cubic box of edge length 10 Å and the first Brillouin zone was sampled at the Gamma-point. The stabilities of Bi substituted GaAs supercells were determined using energies of substitution ( $\Delta E_{sub}$ ) of As atoms (As(g)) with gas-phase Bi atoms (Bi(g)) per substitution:

$$\Delta E_{sub} = \frac{1}{x} (E_{Ga_N As_{N-x} Bi_x} + x E_{As(g)} - E_{Ga_N As_N} - x E_{Bi(g)})$$
(1)

where E values represent DFT derived energies for each structure, subscript N is the numbers of Ga atoms in the GaAs supercell, and subscript x is the number of Bi atoms substituted. Lower  $\Delta E_{Sub}$  values represent more stable Bi configurations in the GaAs lattice. These values are defined per Bi atom to normalize the energies when comparing four and eight Bi atom ensembles studied in this work. The thermodynamic

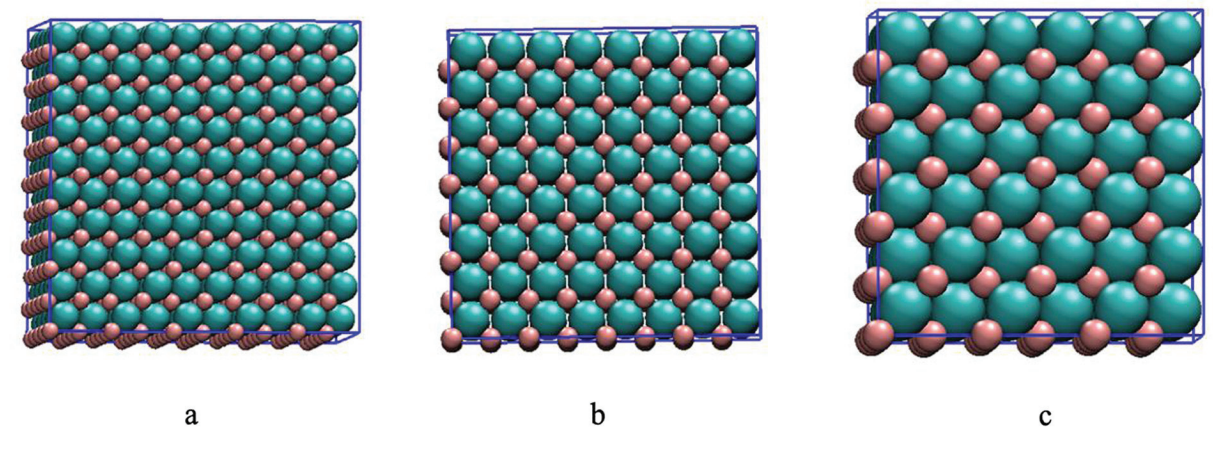


Fig. 1. Supercells containing (a)  $5 \times 5 \times 5$ , (b)  $4 \times 4 \times 4$  and (c)  $3 \times 3 \times 3$  GaAs unit cells used to achieve Bi concentrations shown in Table 1 for GaAsBi compounds. Pink and cyan atoms represent Ga and As, respectively.

clustering preference of groups of atoms can be represented by energies per supercell given by  $4 \times \Delta E_{sub}$  and  $8 \times \Delta E_{sub}$  for four and eight Biatom ensembles, respectively.

Eq. (1) uses energies of isolated atoms As(g) and Bi(g) that represent gaseous species approaching the substrate in molecular beam epitaxy (MBE). The energies of solid-state atoms Bi(s) and As(s) instead represent the stabilities of final states. The energies of these elemental solid states per As or Bi atoms were derived from spin-polarized calculations of their rhombohedral unit cells using a  $10 \times 10 \times 10$  Monkhorst-Pack k-point mesh [23,24] with lattice constants varied in steps of 2% around the experimental values of 4.131 Å for As and 4.746 Å for Bi [29]. The change in energy as a function of lattice constant was fit to a quadratic equation for each crystal to determine the minimum energy of solid-phase As,  $E_{As(s)}$  and solid-phase Bi,  $E_{Bi(s)}$ . These DFT derived lattice constants with minimum energy for As and Bi were 4.205 Å and 4.821 Å which were 1.8% and 1.6% larger than the experimental values, respectively. The comparison of gaseous and solid-state energies is shown in Supporting Information (Table S3). Substituting the energies of As(g) and Bi(g) in Eq. (1) with that of As(s) and Bi(s), respectively, lowers all  $\Delta E_{sub}$  values by 40.21 kJ mol<sup>-1</sup>, suggesting that the incorporation of Bi into GaAs lattice is more favorable for the solid-state reference for the elemental energies. The relative  $\Delta E_{sub}$  values for different Bi configurations in the GaAs supercells remain unchanged with the choice of reference state because all  $\Delta E_{sub}$  values decrease by the same constant value.

#### 3. Results and discussion

# 3.1. Configurations of four Bi atoms in GaAsBi and stabilities at different Bi concentrations

We first calculate the stabilities of specific arrangements of four Bi atoms in  $5\times5\times5$ ,  $4\times4\times4$  and  $3\times3\times3$  supercells. These arrangements are named dispersed, tetrahedral, square planar, zig-zag, planar (101), planar (111), linear [001], linear [101] and linear [111], as shown in Fig. 2 for the  $4\times4\times4$  supercell. The energies of these configurations are also compared to randomly generated configurations.

The dispersed configuration comprises one Bi atom at a corner of the supercell and three near face center positions, leading to the maximum separation between Bi atoms for a given Bi concentration. This configuration represents the most uniform Bi distribution and serves as a reference for comparison with configurations containing aggregated Bi atoms. Table 2 shows the average distances between Bi atoms in the As sub-lattice of GaAs in the dispersed configuration at 0.8%, 1.6%, and 3.7% Bi concentrations. The tetrahedral configuration contains one Bi atom at the corner of the supercell and three in the next nearest (111) plane for the As sub-lattice, which gives the most closely packed threedimensional structure of four Bi atoms. Thus, the difference between dispersed and tetrahedral configurations is considered to reflect a possible clustering preference for Bi atoms with increasing Bi content. Both these configurations involve Bi atoms present across multiple crystallographic planes. The remaining configurations in Fig. 2 represent planar and linear aggregated arrangements. The square-planar and zigzag configurations represent square and parallelogram arrangements, respectively, within a (001) plane, while planar (101) represents a rectangular arrangement in (101) plane and planar (111) contains a rhombus-shaped arrangement in (111) plane. The linear patterns consist of four contiguous Bi atoms in the As sub-lattice along [100], [101] and [111] directions. For the case of the  $3 \times 3 \times 3$ supercell four contiguous Bi atoms could not be accommodated for linear [001] and linear [111] arrangements; therefore, the linear [001] configuration consist of three contiguous Bi atoms and one Bi atom near the center of the supercell while the linear [111] arrangement contains three contiguous Bi atoms and one Bi atom at the supercell corner (structures in Supporting Information, Fig. S4). Table 3 shows distances between contiguous atoms in different line directions in the As sub-lattice of GaAs. The  $[1\,0\,1]$  and  $[1\,1\,1]$  directions are the most and the least densely packed directions, respectively. In contrast, for the planar arrangements the  $(1\,1\,1)$  plane is the most densely packed while  $(1\,0\,1)$  plane is less closely packed.

Energies of ten other configurations formed by Bi substitution at randomly generated combinations of four As atom locations were also calculated. The stability for Bi substitution in random configurations was determined by taking a weighted average given by:

$$\langle \Delta E_{sub} \rangle = \frac{\sum_{i=1}^{10} \Delta E_{sub,i} e^{-\frac{\Delta E_{sub,i}}{RT}}}{\sum_{i=1}^{10} e^{-\frac{\Delta E_{sub,i}}{RT}}}$$
(2)

where  $\langle \Delta E_{sub} \rangle$  is the average substitution energy,  $\Delta E_{sub,i}$  is the substitution energy for each of the random configurations determined form Eq. (1), R is the universal gas constant, and T is the temperature taken here to be 298 K. This random configuration energy was used to determine if arrangements other than the specific configurations in Fig. 2 can be more stable. The point coordinates, structures and energies for all random atom configurations for the  $4 \times 4 \times 4$  supercell are shown in Supporting Information (Fig. S5 and Tables S5a–b).

The substitution energies per Bi atom for the introduction of four Bi atoms in 5  $\times$  5  $\times$  5, 4  $\times$  4  $\times$  4, and 3  $\times$  3  $\times$  3 GaAs supercells at 0.8%, 1.6%, and 3.7% Bi concentrations, respectively, are shown in Fig. 3. Their values range from 142 to  $155\,\mathrm{kJ}\,\mathrm{mol}^{-1}$  for the different Bi atom configurations shown in Fig. 2. These  $\Delta E_{sub}$  values were derived using energies of isolated atoms for As and Bi elements in Eq. (1) to represent the gaseous atoms approaching substrates in molecular beam epitaxy (MBE). The use of solid states of these elements instead lowers all  $\Delta E_{sub}$ values by a constant 40.21 kJ mol<sup>-1</sup> (details in Supporting Information, Section S3), which leads to values ranging from 101 to 115 kJ mol<sup>-1</sup> in Fig. 3 without changing the relative differences for the different configurations. The use of dispersion correction further lowers these substitution energies by 52-53 kJ mol<sup>-1</sup> when gas-phase atoms are used for elemental energies as shown in Eq. (1) (details in Supporting Information, Table S1), because Bi atoms seem to exhibit greater van der Waals (vdW) stabilization than As in the lattice. Analogous preferential vdW stabilization of elemental Bi in solid states of these elements is likely to offset any significant dispersion effects in the net  $\Delta E_{sub}$ values. The dispersion corrections also keep the relative  $\Delta E_{sub}$  differences among the different configurations nearly unchanged (Table S1). Taken together these effects indicate that the absolute  $\Delta E_{sub}$  values remain greater than 50 kJ mol<sup>-1</sup> for most configurations in Fig. 3. These highly positive values represent the metastable nature of Bi in the GaAs lattice, but do not include contributions of lattice vibrational energy [30,31] and configurational entropy [32] to the Gibbs free energy. Such contributions partially stabilize Bi in the lattice due to smaller vibrational frequencies resulting in lower vibrational energies for the heavier Bi atoms as well as many possible degenerate arrangements for various dopant configurations. Therefore, the DFT derived electronic  $\Delta E_{sub}$  values only reflect how relative trends in stabilities of the different configurations change with concentration, instead of absolute stabilities of each.

#### 3.1.1. 0.8% Bi concentration

At 0.8% Bi concentration in the  $5 \times 5 \times 5$  supercell (500 Ga, 4 Bi, 496 As atoms) the substitution energies range from  $142 \, \text{kJ} \, \text{mol}^{-1}$  to  $147 \, \text{kJ} \, \text{mol}^{-1}$ . The dispersed Bi configuration with distant Bi atoms is more stable than the three-dimensional tetrahedral arrangement of Bi clusters by  $1.9 \, \text{kJ} \, \text{mol}^{-1}$  per Bi atom (Fig. 3). Thus, groups of four Bi atoms at 0.8% of group V atoms are more stable in dispersed than in tetrahedral form by  $7.6 \, \text{kJ} \, \text{mol}^{-1}$ . For comparison, the value of thermodynamic reference energy kT at  $500 \, \text{K}$  and  $600 \, \text{K}$  (typical MBE growth temperatures [3,33,34]) is  $4.16 \, \text{and} \, 4.99 \, \text{kJ} \, \text{mol}^{-1}$ , respectively. Thus the  $7.6 \, \text{kJ} \, \text{mol}^{-1}$  preference for dispersed configuration is thermodynamically significant. The equilibrium constant for

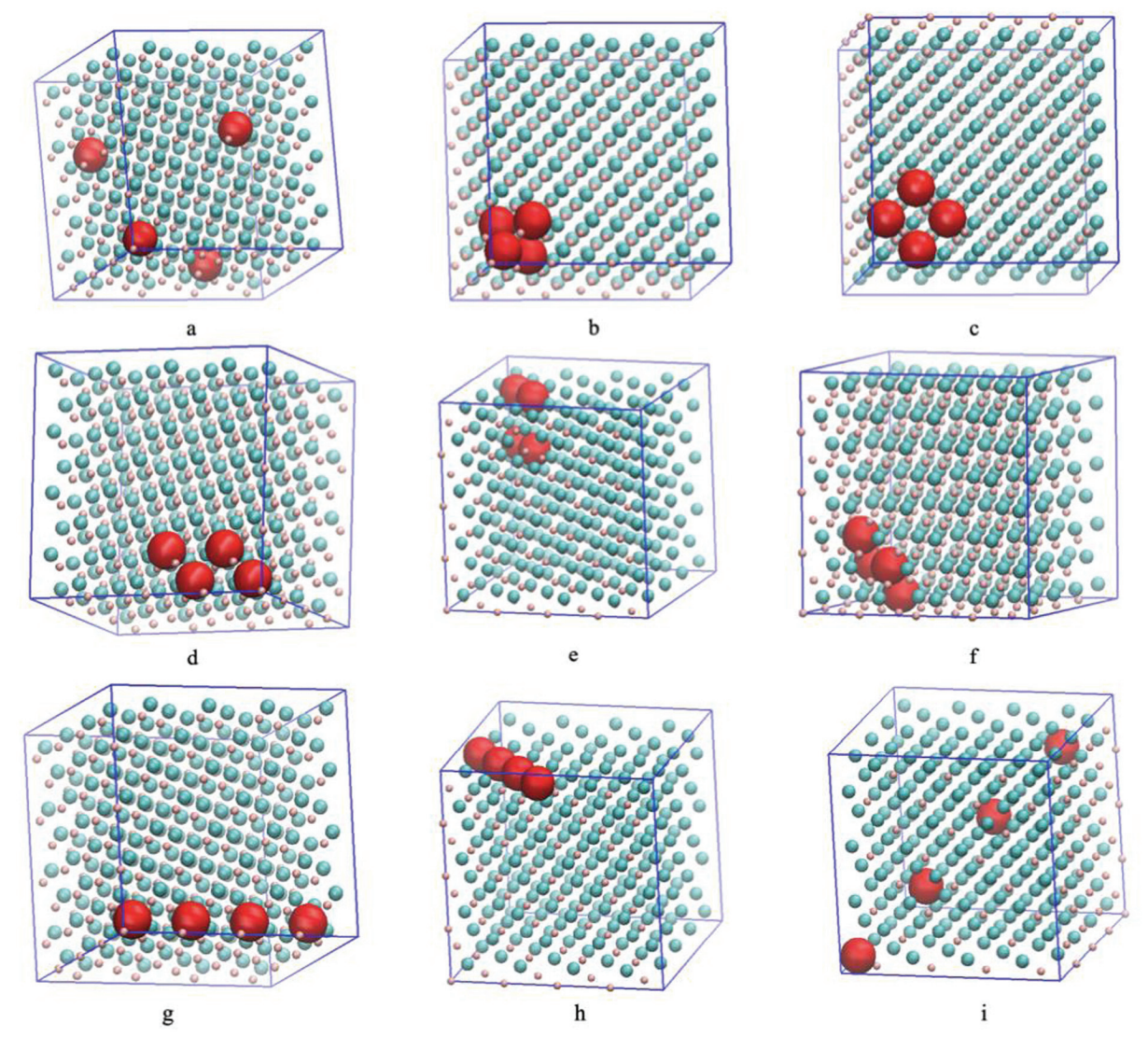


Fig. 2. (a) Dispersed, (b) tetrahedral, (c) square planar, (d) zigzag, (e) planar (101), (f) planar (111), (g) linear [100], (h) linear [101] and (i) linear [111] structural configurations for 1.6% Bi in a  $4 \times 4 \times 4$  GaAs supercell. Analogous patterns were implemented for  $3 \times 3 \times 3$  and  $5 \times 5 \times 5$  supercells with 3.7% and 0.8% Bi, respectively. Red, cyan and pink atoms represent Bi, As, and Ga, respectively.

 Table 2

 Average distances between Bi atoms in As sub-lattice in the dispersed configurations.

Bi concentration (%)	Average Bi – Bi distances (Å)
0.8	20.43
1.6	16.35
3.7	12.26

 $\begin{tabular}{ll} \textbf{Table 3} \\ \textbf{Distances between contiguous atoms in As sub-lattice for lines in different directions.} \\ \end{tabular}$ 

Line direction	Reference structure in Fig. 2	Alignment	Contiguous atom distance (Å)
[100]	2(g)	Cube edge	5.78
[101]	2(h)	(parallel to) face diagonal	4.09
[111]	2(i)	Body diagonal	10.01
[221]	Not shown	Origin to opposite face center	7.08

interconversion among these two configurations is 6.2 and 4.5 at 500 K and 600 K, respectively, in favor of the dispersed state ( $K_{eq} = \exp(-\Delta E/RT)$ ). The energy differences among various other configurations discussed in later parts of this manuscript is larger and more thermodynamically significant (Fig. 3). In particular, the stability preference for linear [101] and planar (111) becomes particularly strong at high Bi concentrations.

This difference between dispersed and tetrahedral configurations suggests that Bi atoms exhibit some preference for staying apart at low Bi concentrations. The planar and linear aggregated configurations, however, are even more stable than the dispersed configuration by up to 1.4 kJ mol<sup>-1</sup>, suggesting that even at such low concentrations the Bi atoms may align along a line or a plane but do not prefer to form three dimensional aggregates. At this concentration linear configurations are slightly more stable than planar configurations. The linear [1 0 0] configuration is the most stable one, followed by linear [1 1 1] and linear [1 0 1] (Fig. 3; 1.4, 1.3, and 0.7 kJ mol<sup>-1</sup> lower energy than dispersed). These lines do not correlate with the nearest-neighbor distances for the different line directions (Table 3). However, the more closely packed lines in [1 0 1] direction also contains smaller fractions of the atoms in that line substituted with Bi. The [1 0 1] line can fit ten

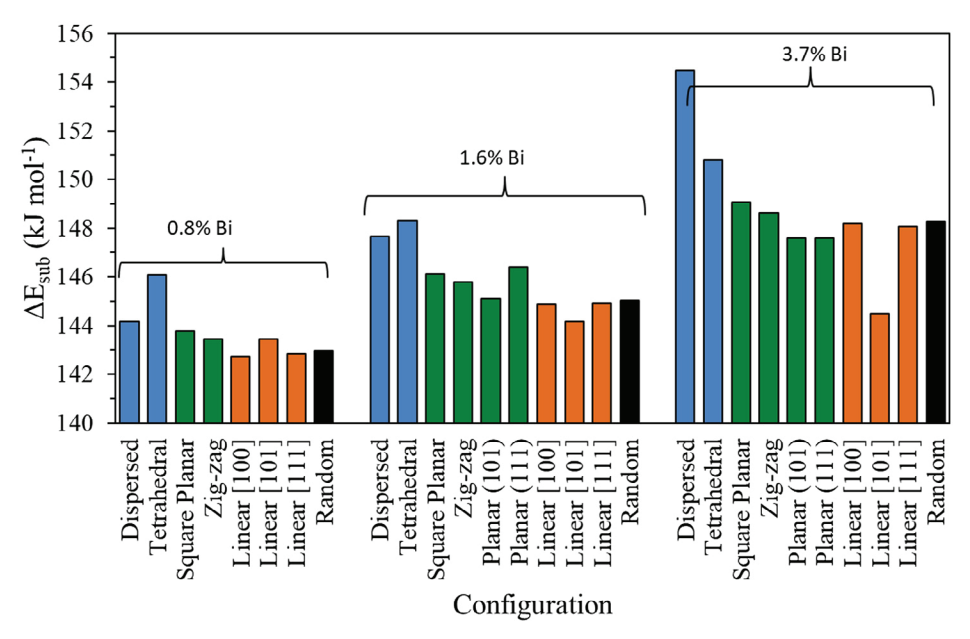


Fig. 3. DFT derived substitution energies per Bi atom ( $\Delta E_{sub}$ ) for different configurations of four Bi atoms in 5 × 5 × 5, 4 × 4 × 4, and 3 × 3 × 3 GaAs supercells (0.8%, 1.6%, and 3.7% Bi concentrations, respectively). The energies for random configuration represent a weighted average of ten configurations as defined by Eq. (2). Blue, green, orange and black bars represent three-dimensional, planar, linear and random configurations, respectively.

atoms within a 5  $\times$  5  $\times$  5 supercell, only four of which are Bi atoms at 0.8% concentration. In contrast, the [1 0 0] and [1 1 1] lines contain five atoms within the supercell, four of which are Bi. These linear patterns are repeated due to periodic boundary conditions, leading to more complete continuous line in [1 0 0] and [1 1 1] directions. We surmise that GaAsBi lattices can relax linear strain sources originating from larger Bi atoms in a line better than three dimensional ones with multiple points of strain origination in periodic lattice, and the nearest-atom spacing as well as the completeness of the lines may matter for stability. In general, the differences between different linear and planar arrangements are small at 0.8% Bi, and we revisit these trends at greater Bi concentrations in the following discussions, where some aggregation preferences become more prominent.

The weighted average of the  $\Delta E_{sub}$  values for ten configurations selected by random sampling is significantly lower than dispersed and tetrahedral configurations but about 0.3 kJ mol<sup>-1</sup> higher than the linear [100] configuration that was most stable of all configurations in Fig. 2 at 0.8% Bi. Low energy configurations contribute much more significantly to these weighted averages (Eq. (2)), and, therefore, the averages represent values near the minimum of all sampled random configurations. The structures and energies of the most stable configurations among the randomly selected ones at different Bi concentrations and their energies are shown in Supporting Information (Fig. S6 and Table S6). For 0.8% Bi, the most stable configuration among the randomly selected ones has nearly identical energy to the linear [100] configuration, (within 0.05 kJ mol<sup>-1</sup>). These lowest energy configurations for all Bi concentrations invariably contain a few atom-pairs with spacings within the nearest-neighbor distances shown in Table 3, suggesting that some extent of Bi aggregation is factored into the "average random energies," shown in Fig. 3. Therefore, these average energies cannot act as a reference state to gauge the clustering preferences of Bi atoms, and the dispersed configuration in Fig. 2 is a more appropriate reference. Nonetheless, the linear [100] energies are similar to the most stable of the random configuration, suggesting that there is no significant preference for any of the specific well-ordered aggregated configurations over randomly selected partially aggregated ones. Conversely, none of the random ones are much more stable than linear [100], therefore, no other configurations that yield significantly greater stability than the sampling of configurations performed in Fig. 2 were found by random guesses.

Analogous studies on configurational preferences for groups of two, three and four atoms were performed by Bannow et al. [35]. These studies utilized supercells with 8, 27 and 64 Ga atoms based on multiples of two-atom primitive unit cells of rhombohedral shape in contrast to the eight-atom cubic unit cells used here. As a result, their Bi concentrations for four Bi-atom configurations were much larger than the concentrations used here (128, 256 and 500 Ga atoms; Table 1), and the linear arrangements and directions do not correspond to the directions reported here. Nonetheless, the studies of Bannow et al. also show that tetrahedral arrangements are less stable than linear arrangements, as shown by our results in Fig. 3. The random configuration energy included in their approach was derived from a "special quasirandom structures" approach [36] which samples various pairwise interactions but not periodic interactions, which can be very significant in small supercells, and do not correspond to the averages of the random configurations reported here.

#### 3.1.2. 1.6% Bi concentration

At 1.6% Bi concentration in the  $4 \times 4 \times 4$  supercell, the substitution energies ( $\Delta E_{sub}$ ) range from 144 kJ mol<sup>-1</sup> to 149 kJ mol<sup>-1</sup> for the different Bi atom configurations (Fig. 3). These energies are higher than the energies of the corresponding configurations at 0.8% Bi concentration, which suggests that GaAsBi stabilities decrease with increased concentration. This increase in substitution energies with concentration is not uniform for all configurations. Instead, the dispersed configuration becomes less stable by 3.5 kJ mol<sup>-1</sup> while the aggregated tetrahedral, square planar, zig-zag, linear [100] and [111] and average random configurations were less stable by 2.1–2.3 kJ mol<sup>-1</sup> and linear [1 0 1] by only 0.7 kJ mol<sup>-1</sup>. These differences suggest that the preference to the aggregated arrangements is greater at higher Bi concentrations, consistent with clustering observed at higher Bi concentration in experiments [9]. For three-dimensional arrangements the dispersed configuration, however, remains slightly more stable than the tetrahedral configuration (Fig. 3, 1.6% Bi). Among the planar configurations, (101) is slightly more stable than the square planar, while the planar (111) is slightly less stable than square planar (100) configuration. The (111) planar arrangement when extended further at higher Bi concentrations becomes analogous to Cu-Pt type Bi-As

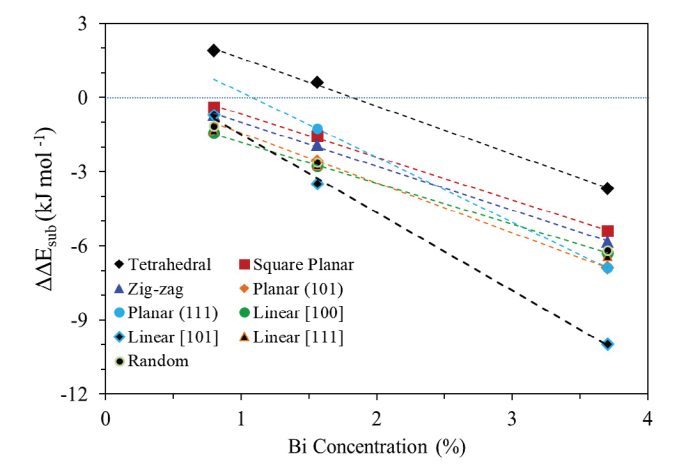


Fig. 4. Difference in Bi atom substitution energies per Bi atom ( $\Delta \Delta E_{sub}$ ) between the aggregated configurations and the dispersed configuration shown in Fig. 2 as a function of Bi concentration. The aggregated configurations include tetrahedral (black diamonds), square planar (maroon squares), zigzag (blue triangles), planar (101) (orange diamonds), planar (111) (light blue circles), linear [100] (green circles), linear [101] (diamonds with light blue borders), linear [111] (triangles with orange borders), and random (circles with green borders). Dashed lines represent linear best fits.

structure observed in experiments at higher Bi concentrations [11]. The lower stability of this structure suggests that the formation of these structures is not favored thermodynamically at low Bi concentrations using ensembles of four Bi atoms that do not allow formation of a large continuous platelet along the (1 1 1) plane.

Among the linear arrangements, [101], which was less stable than [1 0 0] and [1 1 1] at 0.8% Bi is more stable than these two at 1.6% Bi by 0.7 and 0.8 kJ mol<sup>-1</sup>, respectively. As noted previously, for 0.8% the [1 0 1] line is incomplete with only four of ten atoms as Bi. At 1.6% Bi in  $4 \times 4 \times 4$  supercell, this line becomes more complete with four As and four Bi atoms in the [101] line. The [100] and [111] lines also become fully complete with all four atoms in the unit cell occupied by Bi and extended by periodic neighbors. The [101] line with closer nearest-neighbor distances (Table 3) becomes more stable than other directions as this line becomes more complete. This trend continues at higher concentrations discussed next. The average (Eq. (2)) and the most stable Bi substitution energies for randomly generated configurations are 0.9 and 0.6 kJ mol $^{-1}$  higher than the linear [101], suggesting that a preference for well-ordered linear arrangement in the most closely packed direction emerges even over randomly generated partially-ordered configurations as Bi concentration increases. These clustering preferences remain unchanged when dispersion correction is applied (details in Supporting Information, Table S1), because even in this case, tetrahedral configuration is less stable than dispersed, and planar (111) and linear [101] are more stable, with the latter being the most stable.

### 3.1.3. 3.7% Bi concentration

At 3.7% Bi concentration in the  $3 \times 3 \times 3$  supercell, the  $\Delta E_{sub}$  values per Bi atom range from  $144.5 \, \text{kJ} \, \text{mol}^{-1}$  to  $155 \, \text{kJ} \, \text{mol}^{-1}$  for different Bi atom configurations (Fig. 3). Most of these energies are much higher than the corresponding values at 0.8% and 1.6% Bi, consistent with a decrease in GaAsBi stability with increasing Bi content for most configurations. The dispersed and clustered configurations continue to exhibit different sensitivity to Bi concentration, leading to more stable tetrahedral configuration than dispersed at  $3.7 \, \text{kB}$ . The  $\Delta E_{sub}$  value for the tetrahedral geometry is  $3.7 \, \text{kJ} \, \text{mol}^{-1}$  lower than that for the dispersed, which confirms that Bi clustering preference continues to increase with increasing Bi concentration. The square planar, zig-zag, planar (1 0 1), and linear [1 0 0] and [1 1 1] configurations remain more

stable than tetrahedral and show similar relative stabilities as that for 1.6% Bi. The planar ( $1\,1\,1$ ), which was less stable then planar ( $1\,0\,1$ ) at 1.6% becomes nearly as stable, suggesting a slight increase in stability for configurations with Bi atoms on the ( $1\,1\,1$ ) planes at higher Bi concentrations.

Among the linear configurations, [100] and [111] exhibit similar  $\Delta E_{sub}$  values, while this value for [1 0 1] is lower than the two by 3.7 and 3.6 kJ mol<sup>-1</sup>, respectively, suggesting very high stability for the linear [1 0 1] configuration (Fig. 3). At 3.7% Bi in  $3 \times 3 \times 3$  supercell, the [1 0 1] line becomes more complete than lower concentrations with four Bi atoms out of six. The [100] and [111] lines, in contrast, contain only three atoms in this supercell, leading to complete Bi lines and an extra Bi atom to be placed at the farthest possible location to this line and its periodic images. As discussed for lower concentrations, the more complete line and the closest nearest-neighbor distance (Table 3), both potentially contribute to the very high stability of the linear [101] configurations. The extra atom for [100] and [111] linear configurations possibly contributes to their instability. The linear [101] configuration at 3.7% Bi is also more stable than the weighted average energies (Eq. (2)) of randomly selected configurations, by 3.8 kJ mol<sup>-1</sup>, suggesting much more significant preference to well-ordered linear alignment along most closely packed direction than partially aggregated random configurations at these Bi concentrations.

#### 3.1.4. Effect of concentration on clustering preferences

The clustering preferences indicated by the energies in Fig. 3 are summarized by the difference in the  $\Delta E_{sub}$  values between each configuration and the most highly dispersed configuration:

$$\Delta \Delta E_{sub} = \Delta E_{sub} - \Delta E_{sub, dispersed} \tag{3}$$

These  $\Delta\Delta E_{sub}$  values for tetrahedral, square planar, zig-zag, planar (101) and (111), linear [100], [101], and [111], and average energies of random configurations are shown as a function of Bi concentration in Fig. 4.

The  $\Delta \Delta E_{sub}$  values for all configurations decrease monotonically and nearly linearly with Bi concentration, which is consistent with significantly enhanced preference to form Bi clusters at higher concentrations (Fig. 4). At 0.8% Bi, the tetrahedral configuration is less stable than the dispersed one with uniformly spread Bi atoms, while square planar, zig-zag and linear ones are slightly more stable. At concentrations above 2%, all clustered configurations including tetrahedral become more stable than the dispersed one. The  $\Delta\Delta E_{sub}$  values change from +1.9 to -1.4 kJ mol<sup>-1</sup> for tetrahedral, from -3.7 to -6.3 kJ mol<sup>-1</sup> for linear [1 0 0] and from -0.7 to -10.0 kJ mol<sup>-1</sup> for linear [101] configurations. The relative stability among most clustered arrangement changes weakly with Bi concentration. For example, the difference between  $\Delta \Delta E_{sub}$  values for the tetrahedral clusters to the linear arrangement decreases only from 3.3 kJ mol<sup>-1</sup> at 0.8% Bi to 2.6 kJ mol<sup>-1</sup> at 3.7% Bi, suggesting that the instability of the tetrahedra relative to lines is decreasing only slightly with increasing concentration. The weighted average energy of randomly selected configurations is very similar to that of linear [100] configuration at all three Bi concentrations. However, the stabilities of planar (111) and linear [101] arrangements, both involving most dense packing in a plane or along a line, increase more sensitively than aggregated configurations with increasing Bi concentration (as indicated by slopes in Fig. 4). At 3.7% Bi the linear [1 0 1] configuration becomes much more stable than all configurations.

These results suggest that the relaxation of the GaAs lattice in response to the local strain imposed by the replacement of As atoms with much larger Bi atoms is more efficient if the larger atoms are grouped together instead of distributed origins of strains. For the grouped atoms, the relaxations are more efficient for linear or planar strains than three dimensional ones, and configurations involving more densely packed (1 1 1) planes and [1 0 1] lines become more stable than others at 3.7% Bi or larger. These computational results are consistent with

experimental growth results of GaAsBi compounds using MBE which have shown that Bi atoms preferentially bind at planar sites of GaAs, particularly the  $(0\,0\,1)$  plane [17]. They are also consistent with atomic resolution electron microscopy and DFT studies showing preference for linear ordering along [100] and [101] linear directions [16]. The stability of these linear arrangements was traced to the stabilization by stronger Bi-Ga bonds for adjacent Bi atoms with in-plane Ga atoms relative to those for isolated Bi atoms.

Next, we look at the effects of changing the Bi concentrations by increasing the Bi ensemble size in the  $4\times4\times4$  GaAs supercell from four to eight Bi atoms. These larger ensembles lead to additional planar and three-dimensional arrangements, some of which are significantly more stable than the linear arrangements that were found to be most stable for configurations involving four Bi atoms.

# 3.2. Configurations and stabilities of eight Bi atoms in 4 $\times$ 4 $\times$ 4 supercell at 3.1% Bi concentration

To accommodate eight Bi atoms in a  $4 \times 4 \times 4$  GaAs supercell without deviating from arrangements for four Bi atoms, two categories of GaAsBi systems comprising eight Bi atoms were examined. These configurations are shown in Figs. 5 and 6. The first type of system consists of a fixed Bi tetrahedron near the center of the supercell accounting for four Bi atoms and the remaining four Bi atoms were arranged in dispersed, square planar, zigzag and linear [100] configurations such that their distances from the central tetrahedron were maximized (Fig. 5). The second type of system contained four Bi atoms in a dispersed arrangement, i.e., one Bi atom at a corner and three Bi atoms near face centers, and the remaining four Bi atoms were arranged in dispersed, square planar, zigzag and linear [100] configurations with maximum separations from the reference dispersed structure (Fig. 6). Fig. 6a corresponds to a dispersed configuration superimposed on another dispersed configuration yielding the maximum separation among Bi atoms for an eight-atom ensemble. The average distances among Bi atoms in this arrangement is 15.98 Å.

Nine additional configurations examined for eight Bi atoms are shown in Fig. 7. One such configuration involved Bi tetrahedra grown

near two of the four edges of the tetrahedron formed by the first four atoms, which leads to a densely packed three-dimensional configuration in which the Bi atoms are as close as possible (Fig. 7a). Four other configurations targeted planar arrangements, one involving the dispersion of eight Bi atoms as two adjacent lines within a (0 0 1) plane (Fig. 7b), the second having a similar dispersion of eight Bi atoms as two adjacent lines within the (1 0 1) plane (Fig. 7c), the third involving dispersion of eight Bi atoms as two adjacent lines within the (1 1 1) plane (Fig. 7d), and the fourth having eight Bi atoms aggregated in a (1 1 1) plane (Fig. 7e). These configurations are denoted planar (1 0 0), planar (1 0 1), planar (1 1 1) v1 and planar (1 1 1) v2, respectively.

The remaining four configurations probed linear arrangements of eight Bi atom ensembles. Fig. 7f shows a configuration involving two Bi lines in the [1 0 0] direction occupying As sites in the GaAs lattice such that the distance between the two lines was maximized by introducing one line of Bi atoms at the corner of a (001) plane and another line of Bi near the center of the GaAs supercell. Fig. 7g and 7 h depict linear configurations in which eight Bi atoms are aligned along the [101] crystallographic direction. Fig. 7g involves a single line of eight Bi atoms in the [101] direction occupying As sites in the GaAs lattice while Fig. 7h involves two lines of Bi atoms occupying As sites in the GaAs lattice along the [101] direction by having one line of four Bi atoms near the corner of a (001) plane in the [101] direction while another line of four Bi atoms near the center of the GaAs supercell in the [101] direction such that the distance between the two lines was maximized. The final linear configuration shown in Fig. 7i involves two Bi lines in the [1 1 1] direction at As sites in the GaAs lattice such that the separation between the two lines was maximized by introducing one line of Bi atoms along the body diagonal of the GaAs supercell and the other [1 1 1] line of Bi atoms near the corner of the GaAs supercell (see Supporting Information for a better visual representation of linear [111] configuration with unit cell repeating periodically in all three directions, Fig. S7). In addition to the configurations shown in Figs. 5–7, energies of ten other configurations formed by Bi substitution at randomly generated combinations of eight As atom locations was calculated. The weighted average of the energies of these random configurations was calculated using Eq. (2).

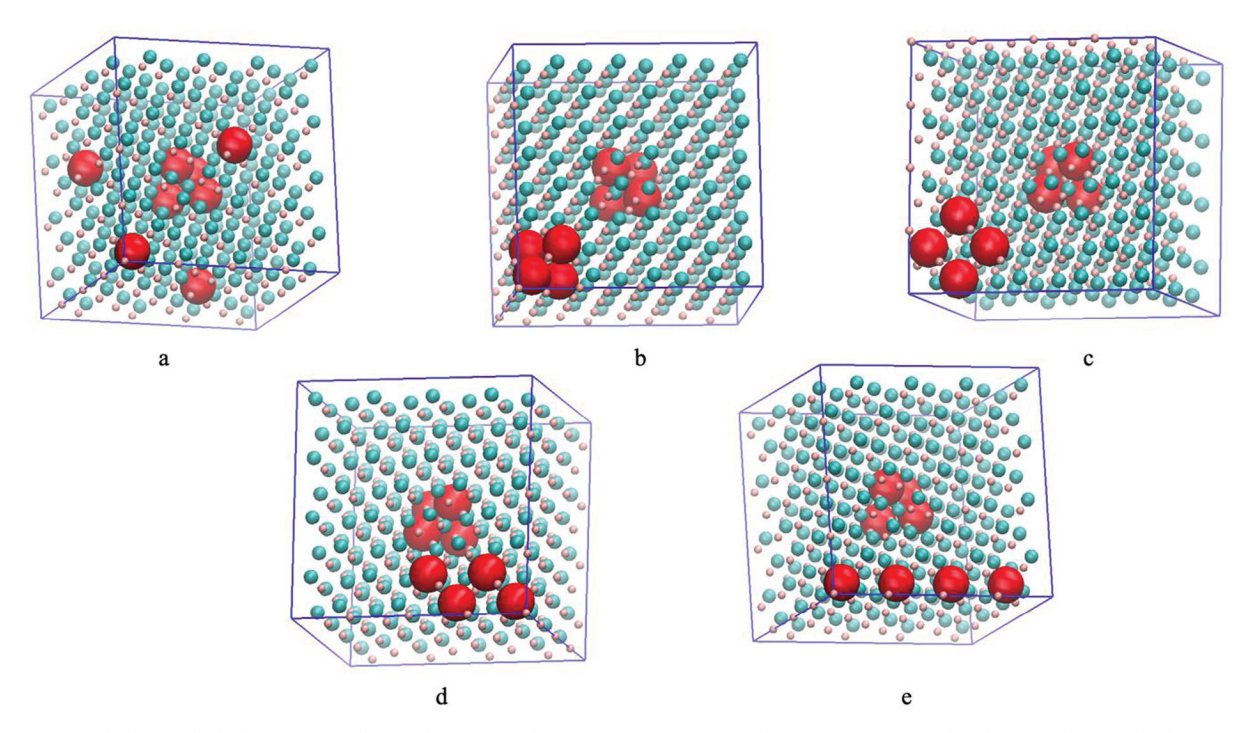


Fig. 5. (a) Dispersed, (b) Tetrahedral, (c) Square Planar, (d) Zigzag, and (e) Linear [1 0 0] structural configurations paired with a central Bi tetrahedron for 3.1% Bi in a 4 × 4 × 4 GaAs supercell. Red, cyan and pink atoms represent Bi, As, and Ga, respectively.

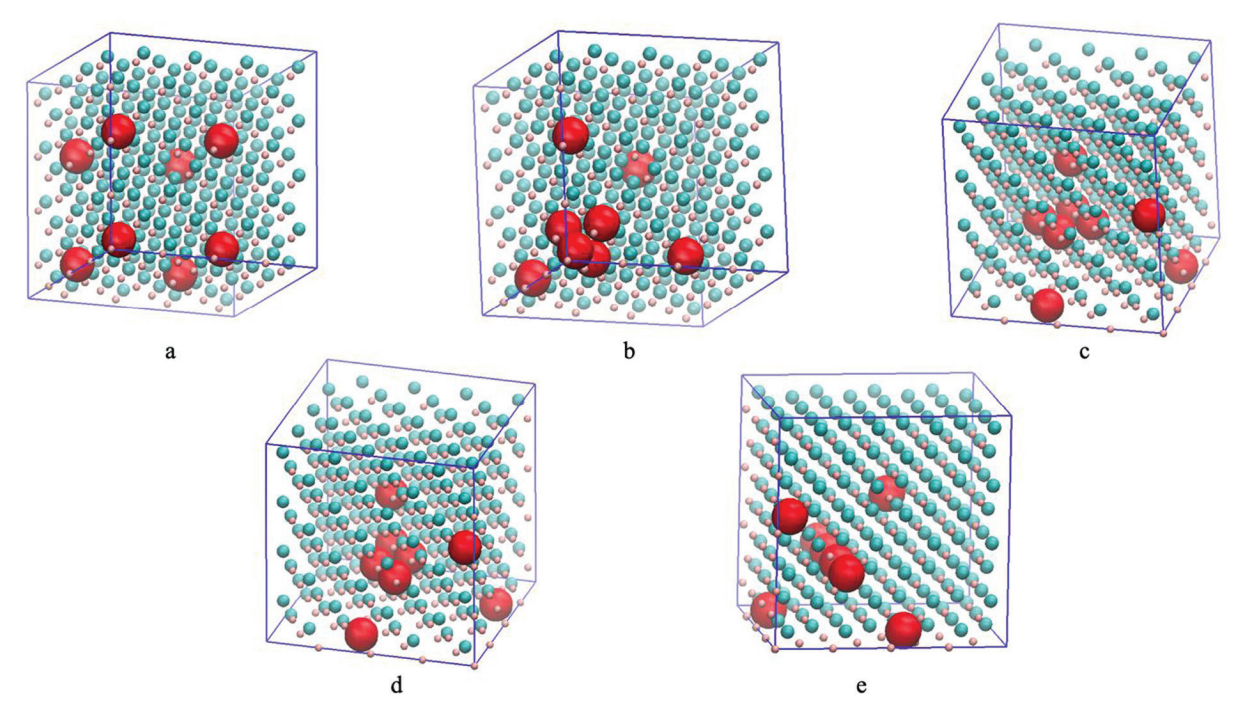


Fig. 6. (a) Dispersed, (b) Tetrahedral, (c) Square Planar, (d) Zigzag, and (e) Linear [1 0 0] structural configurations paired with four dispersed Bi atoms for 3.1% Bi in a 4 × 4 × 4 GaAs supercell. Red, cyan and pink atoms represent Bi, As, and Ga, respectively.

Fig. 8 shows the substitution energies per Bi atom for the introduction of eight Bi atoms in a  $4 \times 4 \times 4$  GaAs supercell, which corresponds to a 3.1% Bi concentration. This concentration is in between those for four Bi atoms in  $4 \times 4 \times 4$  and  $3 \times 3 \times 3$  supercells (1.6% and 3.7% Fig. 3). The substitution energies for these configurations range from 141 to 149 kJ mol<sup>-1</sup>, which is similar to the values for the 1.6% concentration (144–149 kJ mol<sup>-1</sup>), but with some configurations having even lower energies, and lower than that for 3.7% concentration (147–155 kJ mol<sup>-1</sup>) with four Bi atoms.

The GaAsBi systems containing dispersed, tetrahedral, square planar, zigzag and linear configurations around a central Bi tetrahedron in Fig. 8 exhibit similar stability trends as the configurations without the central tetrahedron for 1.6%Bi in Fig. 3. In both systems, tetrahedral clusters are less stable than the dispersed configuration, but the arrangements of four Bi atoms on the (001) planes are more stable, with the linear [100] configuration being the most stable. The absolute energy of the linear [100] configuration near the central tetrahedron  $(147.2\,kJ\,mol^{-1},\;Fig.\;8)$  is larger than that in  $4\times4\times4$  supercell without the tetrahedron (144.9 kJ mol<sup>-1</sup>, Fig. 3), consistent with the lower Bi concentration in the latter systems. The configuration with two tetrahedra (148.3 kJ mol<sup>-1</sup>, Fig. 8), however, is as stable as a single tetrahedron in the  $4 \times 4 \times 4$  supercell (148.3 kJ mol<sup>-1</sup>, Fig. 3), despite higher Bi concentration for two tetrahedra. These differences likely result from the different orientations of the two tetrahedra that evidently relax more in response to the lattice strain than the periodically repeating units of same tetrahedron.

The  $\Delta E_{sub}$  values shown in Fig. 8 for GaAsBi systems containing dispersed and tetrahedral configurations near a fixed dispersed arrangement of four Bi atoms (Fig. 6ab) are slightly lower than the corresponding configurations around a central tetrahedron (Fig. 5ab). In contrast, the  $\Delta E_{sub}$  values for square planar, zigzag and linear [1 0 0] configurations are slightly higher than a fixed dispersed arrangement. As a result, all the configurations with the fixed dispersed arrangement have very similar energies near 148 kJ mol<sup>-1</sup>. The dispersed configuration superimposed with another dispersed configuration leads to a cubic sub-lattice of Bi atoms (Fig. 6a), which differs significantly from the fcc sub-lattice of the four atom dispersed arrangements (Fig. 2a).

The fcc dispersed arrangement at 1.6% has nearly identical stability as the cubic dispersed arrangement at 3.1% Bi ( $\Delta E_{sub}$  147.7 kJ mol<sup>-1</sup>; Figs. 3, 8) despite higher Bi concentration in the latter system. The linear [1 0 0] configuration is slightly less stable than other planar configurations because the atoms in the linear arrangement here interact closely with the superimposed dispersed arrangement (Fig. 6e). The average stability of these configurations is similar to the configuration with a central tetrahedron.

An additional configuration of eight atoms in  $4 \times 4 \times 4$  supercell involves a three-dimensional close packed cluster (Fig. 7a). The  $\Delta E_{sub}$  value for this cluster is  $147.1 \, \text{kJ mol}^{-1}$ , which is  $0.1 \, \text{kJ mol}^{-1}$  lower than the linear [100] configuration with a central tetrahedron and  $0.7 \, \text{kJ mol}^{-1}$  lower than the linear [100] configuration with four fixed dispersed Bi atoms. These differences suggest that the stability of three-dimensional clusters is similar in energy to the ensembles with some aggregation and linearity but lower than the ensembles comprising linearity paired with dispersion at these concentrations as shown in Fig. 8. However, this three-dimensional configuration is much less stable than the configurations consisting of all planar and linear structures discussed next.

The planar (1 0 0) structure consisting of adjacent [1 0 0] lines and the linear structure with distant [1 0 0] lines at 3.1% Bi (Fig. 7b and 7f) exhibit  $\Delta E_{sub}$  values of  $145.6 \, \text{kJ mol}^{-1}$  and  $146.1 \, \text{kJ mol}^{-1}$ , respectively. These energies are much lower than all eight atom configurations in Figs. 5 and 6, and only slightly less stable than a single line at 1.6% Bi (144.9 kJ mol<sup>-1</sup>, Fig. 3). These results suggest that planar and linear arrangements are favored over three dimensional ones even for eight atom ensembles. Moreover, multiple lines prefer to be adjacent to create a planar structure because the lattice strain introduced by a single Bi line creates additional space in vicinal locations. The weighted average substitution energy of ten random eight atom configurations is close to that for adjacent lines (145.6 kJ mol<sup>-1</sup>). These values are consistent with the trends for four atom configurations that led to linear configuration energies similar to the most stable random configurations.

The  $[1\ 0\ 1]$  lines that were used to form planar  $(1\ 0\ 1)$ , planar  $(1\ 1\ 1)$  v1, a single eight atom line (linear  $[1\ 0\ 1]$  v1) and distant lines (linear

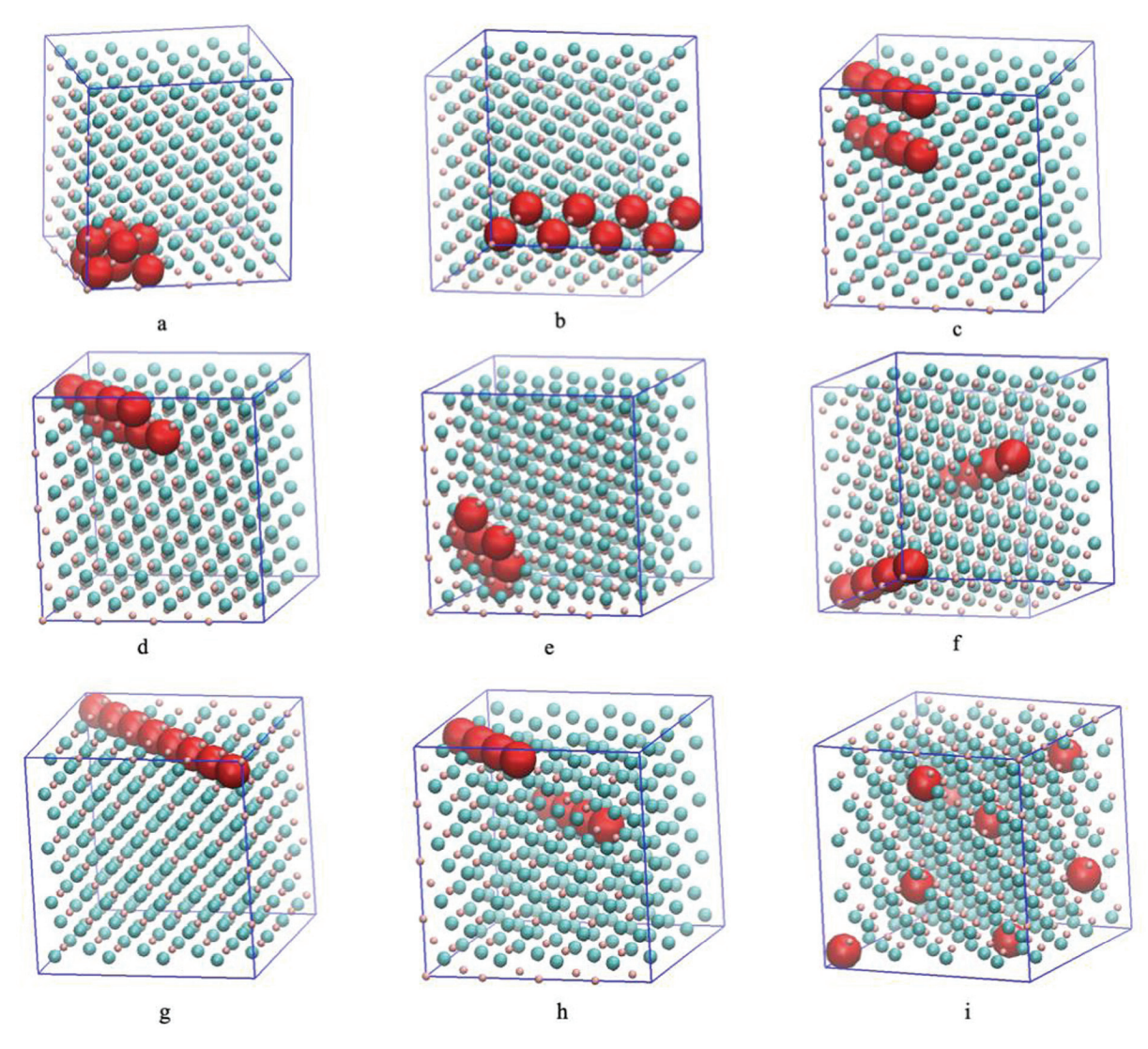


Fig. 7. Additional (a) three-dimensional, (b) planar  $(0\,0\,1)$  (c) planar  $(1\,0\,1)$ , (d) planar  $(1\,1\,1)$  v1, (e) planar  $(1\,1\,1)$  v2, (f) linear  $[1\,0\,0]$ , (g) linear  $[1\,0\,1]$  v1, (h) linear  $[1\,0\,1]$  v2, and (i) linear  $[1\,1\,1]$  structural configurations for 3.1% Bi in a  $4\times4\times4$  GaAs supercell. Additional representation of linear  $[1\,1\,1]$  configuration is shown in the Supporting Information (Fig. S7). Analogous patterns of three-dimensional, planar  $(1\,0\,1)$ , planar  $(1\,1\,1)$  v1, and linear  $[1\,0\,1]$  v1 were implemented for 1.6% Bi in a  $5\times5\times5$  supercell. Red, cyan and pink atoms represent Bi, As, and Ga, respectively.

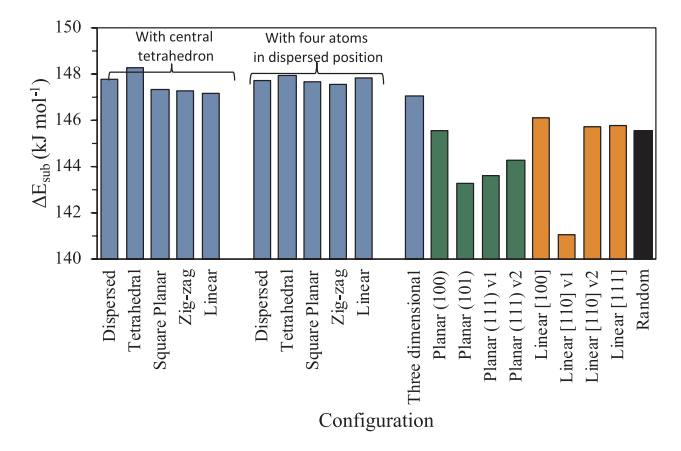


Fig. 8. DFT derived substitution energies ( $\Delta E_{sub}$ ) for different configurations of eight Bi atoms in 4 × 4 × 4 GaAs supercell (3.1% Bi concentration). The energies for random configuration represent a weighted average of ten configurations as defined by Eq. (2).

[101] v2; Fig. 7c, d, f, g) exhibit  $\Delta E_{sub}$  values of 143.3 kJ mol<sup>-1</sup>,  $143.6 \text{ kJ mol}^{-1}$ ,  $141.1 \text{ kJ mol}^{-1}$ , and  $145.8 \text{ kJ mol}^{-1}$ , respectively. The distant [101] lines are 0.3 kJ mol<sup>-1</sup> more stable than the distant [100] lines, but the structures are much more stable. In particular, the single continuous [101] line is much more stable than any of the structures examined including those at the lowest 0.8% Bi concentration. As noticed for 4 atom configurations, the stability of a linear structure depends on the continuity of the lines as well as the spacing between nearest neighbors. The [101] line with closest nearestneighbor Bi distances becomes increasingly more stable as the line becomes more complete for increasing concentrations with 4 Bi atom configurations (Fig. 4). These factors continue to play a role in 8 atom configurations, where a complete 8-atom continuous line repeating with periodic neighbors leads to the most stable of all configurations. This observation is also consistent with the stable [101] line observed in experiments [16]. The planar (101) and the planar (111) v1 structures have similar energies while the planar (111) v2 configuration with less continuous [101] lines is slightly less stable ( $\Delta E_{sub}$ ,  $144.3 \text{ kJ mol}^{-1}$ , Fig. 8).

The  $(1\,1\,1)$  plane represents the most closely packed crystallographic plane in the zinc blende structure, while the  $[1\,0\,1]$  line is the

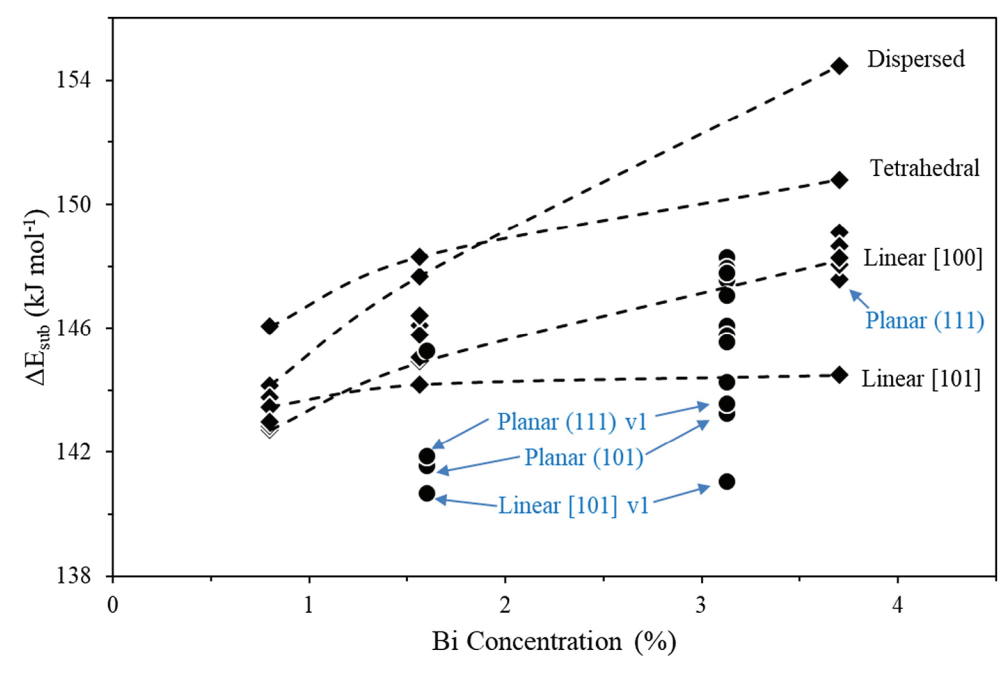


Fig. 9. DFT derived substitution energies per Bi atom ( $\Delta E_{sub}$ ) as a function of Bi concentration for all configurations of four Bi atoms in Fig. 3 (diamonds) and configurations of eight Bi atoms in a 4 × 4 × 4 supercell (circles; 3.1% Bi; structures in Fig. 8) as well as three-dimensional, planar (1 0 1), planar (1 1 1) v1, and linear [1 0 1] v1 configurations of eight Bi atoms in a 5 × 5 × 5 supercell (circles; 1.6% Bi). Dashed curves represent trends in energies of linear [1 0 1], linear [1 0 0], tetrahedral, and dispersed configurations of four-atom ensembles.

most closely packed line. The planar (111) v1 and the linear [101] configurations are more stable than the weighted average energy of the randomly generated configurations by 2.0 kJ mol<sup>-1</sup> and 4.5 kJ mol<sup>-1</sup>, respectively. Thus, for these concentrations and sufficiently large ensemble sizes, the close packed arrangements become significantly preferred over other configurations. These results contrast the four Bi atom configurations, where the stability of planar (111) and linear [101] structures increased with increasing Bi concentration, but even at 3.7% Bi (greater than 3.1% Bi for eight atoms), the planar (111) and linear [1 0 1] configurations were only 0.7 and 3.8 kJ mol<sup>-1</sup> more stable than random, respectively. These results suggest that both concentrations and ensemble sizes matter for stability of close packed configurations. Small patches of (111) planes are relatively unstable even at high concentrations but when large ensemble sizes aggregate, they prefer to align in (111) plane. The arrangements along (111) plane likely becomes even more stable with higher Bi concentration and larger Bi ensembles, leading to experimentally observed CuPt type structures.

#### 3.3. Influence of Bi concentration and ensemble size on stability

Fig. 9 summarizes the effects of Bi concentration and ensemble size on  $\Delta E_{sub}$  values that represent the stability of GaAsBi compounds. The stabilities of four-atom ensembles decrease with increasing Bi concentration for all configurations except the linear [1 0 1] configuration that remains nearly unchanged from 1.6% Bi to 3.7% Bi. The clustering preference enhanced by higher Bi concentrations is reflected in the more significant decrease in stability of dispersed configurations than the aggregated configurations. The weighted average energy of randomly selected configurations is nearly the same as that of linear [1 0 0] for four atom ensembles at all Bi concentrations. At 0.8% Bi the linear [1 0 0] is the most stable configuration. At 1.6% Bi, linear [1 0 1] is slightly more stable than linear [1 0 0], while planar (1 1 1) is also slightly more stable.

For eight-atom Bi ensembles in the  $4 \times 4 \times 4$  supercell (3.1% Bi), the partially aggregated configurations shown in Figs. 5 and 6 exhibit stabilities consistent with the trends for four atom configurations.

However, the planar and linear configurations containing adjacent four atom lines in [101] direction and continuous eight atom lines are much more stable than trends indicated by four atom ensembles. Thus, the ensemble size exhibits significant influence on the stability of GaAsBi compounds in addition to the Bi concentration and the configurations of same-size ensembles. This effect of Bi ensemble size was further confirmed by probing four configurations of eight-atom Bi ensembles in the  $5\times5\times5$  supercell (1.6% Bi). These configurations were analogous to the three-dimensional, planar (101), planar (111) v1, and linear [101] v1 patterns as shown in Fig. 7 but were formed in a larger supercell. The  $\Delta E_{sub}$  values of these configurations are also shown in Fig. 9 as circles at 1.6% Bi concentration. These  $\Delta E_{sub}$  values ranged from 141 kJ mol<sup>-1</sup> to 145 kJ mol<sup>-1</sup> which is a much lower range than that of the 4-atom Bi ensembles at 1.6% Bi concentration (144–149 kJ mol<sup>-1</sup>). In addition, it is strikingly clear once again that the planar configurations with neighboring [101] lines comprising four Bi atoms as well as the continuous eight-atom Bi line are substantially more stable than the four-atom Bi ensembles at the same concentration. This verifies that effects of ensemble size on the stability of GaAsBi compounds are present even at lower Bi concentrations and eliminates any potential influence of supercell size on the stability of GaAsBi compounds. More detailed analysis of such insights would require examination of larger systems and greater number of configurations and combinations of atoms without the periodic limitation of DFT unit cells. Such simulation can be achieved by extracting information about interactions among different atom pairs and subgroups from current and additional DFT calculations via cluster expansion approach, which can then be used to simulate larger systems more efficiently. Such approaches, however, would need to incorporate long-range interactions of aggregates in addition to the pair and sub-group interactions.

# 4. Conclusions

Periodic DFT calculations are used to analyze stabilities of different configurations of GaAsBi compounds with 0.8–3.7% Bi concentrations and ensembles sizes of four and eight Bi atoms. For four-atom

ensembles, higher Bi concentrations lead to greater stability of aggregated Bi configurations over the uniformly segregated ones. Configurations involving linear arrays along [100] direction are similar to random configurations, slightly more stable than other (001), (101) and (111) planar configurations and much more stable than the three-dimensional clusters. The linear [101] and planar (111) configurations are less stable than linear [100] at low concentrations, but their stabilities decrease less sensitively with concentration than other types of aggregated and randomly sampled configurations, making them most stable at higher concentrations. For the eight-atom ensembles at 3.1% Bi, linear [101] and planar (111) or (101) configurations containing adjacent [101] lines are much more stable than other configurations. These eight-atom configurations may be precursors to the CuPt structure found in experiments and their stability increases with Bi concentration as well as ensemble sizes of Bi atoms. The three-dimensional tetrahedral aggregates considered previously as possible configurations at high Bi concentrations is not preferred at any of the concentrations studied here as the preference changes from axial to planar arrangements.

#### 5. Data availability

The data required to reproduce these findings can be obtained by sending a request to Prashant Deshlahra at prashant.deshahra@tufts.edu.

#### CRediT authorship contribution statement

Husain Adamji: Conceptualization, Data curation, Formal analysis, Writing - original draft, Writing - review & editing. Margaret Stevens: Conceptualization, Formal analysis, Writing - review & editing. Kevin Grossklaus: Conceptualization, Formal analysis, Project administration, Writing - original draft, Writing - review & editing. Thomas E. Vandervelde: Conceptualization, Formal analysis, Funding acquisition, Project administration, Writing - review & editing. Prashant Deshlahra: Conceptualization, Data curation, Formal analysis, Project administration, Resources, Supervision, Writing - original draft, Writing - review & editing.

### **Declaration of Competing Interest**

The authors declare that they have no known competing financial interests or personal relationships that could have appeared to influence the work reported in this paper.

#### Acknowledgements

We gratefully acknowledge financial support from Tufts University, Tufts Summer Scholar grant, and computational resources from Tufts high performance computing center and resources provided by Extreme Science and Engineering Discovery Environment (XSEDE) [37], which is supported by National Science Foundation (grant number ACI-1548562). TEV, KG and MS acknowledge support from Office of Naval Research (grant number N00014-15-1-2946).

## Appendix A. Supplementary data

Supplementary data to this article can be found online at https://doi.org/10.1016/j.commatsci.2019.109401.

## References

- J.A. del Alamo, Nanometre-scale electronics with III–V compound semiconductors, Nature 479 (2011) 317–323.
- [2] E.C. Young, GaNAs and GaAsBi: Structural and Electronic Properties of Two Resonant State Semiconductor Alloys, Text, University of British Columbia, 2006

- https://open.library.ubc.ca/collections/831/items/1.0078563.
- [3] M.A. Stevens, K.A. Grossklaus, J.H. McElearney, T.E. Vandervelde, Impact of rotation rate on bismuth saturation in GaAsBi grown by molecular beam epitaxy, J. Electron. Mater. 48 (2019) 3376–3382, https://doi.org/10.1007/s11664-019-06949-6.
- [4] D. Madouri, A. Boukra, A. Zaoui, M. Ferhat, Bismuth alloying in GaAs: a first-principles study, Comput. Mater. Sci. 43 (2008) 818–822, https://doi.org/10.1016/j.commatsci.2008.01.059.
- [5] S. Tixier, M. Adamcyk, T. Tiedje, S. Francoeur, A. Mascarenhas, P. Wei, F. Schiettekatte, Molecular beam epitaxy growth of GaAs1 – xBix, Appl. Phys. Lett. 82 (2003) 2245–2247, https://doi.org/10.1063/1.1565499.
- [6] R.N. Kini, L. Bhusal, A.J. Ptak, R. France, A. Mascarenhas, Electron Hall mobility in GaAsBi, J. Appl. Phys. 106 (2009) 043705, https://doi.org/10.1063/1.3204670.
- [7] M. Seong, S. Francoeur, S. Yoon, A. Mascarenhas, S. Tixier, M. Adamcyk, T. Tiedje, Bi-induced vibrational modes in GaAsBi, Superlattices Microstruct. 37 (2005) 394–400, https://doi.org/10.1016/j.spmi.2005.02.004.
- [8] Z. Jiang, D.A. Beaton, R.B. Lewis, A.F. Basile, T. Tiedje, P.M. Mooney, Deep level defects in GaAs1 – xBix/GaAs heterostructures, Semicond. Sci. Technol. 26 (2011) 055020, https://doi.org/10.1088/0268-1242/26/5/055020.
- [9] G. Ciatto, E.C. Young, F. Glas, J. Chen, R.A. Mori, T. Tiedje, Spatial correlation between Bi atoms in dilute GaAs1-xBix From random distribution to Bi pairing and clustering, Phys. Rev. B 78 (2008) 035325, https://doi.org/10.1103/PhysRevB.78. 035325.
- [10] D.L. Sales, E. Guerrero, J.F. Rodrigo, P.L. Galindo, A. Yáñez, M. Shafi, A. Khatab, R.H. Mari, M. Henini, S. Novikov, M.F. Chisholm, S.I. Molina, Distribution of bismuth atoms in epitaxial GaAsBi, Appl. Phys. Lett. 98 (2011) 101902, https://doi. org/10.1063/1.3562376.
- [11] A.G. Norman, R. France, A.J. Ptak, Atomic ordering and phase separation in MBE GaAs1 – xBix, J. Vac. Sci. Technol., B 29 (2011) 03C121, https://doi.org/10.1116/ 1.3562512.
- [12] A. Janotti, S.-H. Wei, S.B. Zhang, Theoretical study of the effects of isovalent coalloying of Bi and N in GaAs, Phys. Rev. B 65 (2002) 115203, https://doi.org/ 10.1103/PhysRevB.65.115203.
- [13] Y. Zhang, A. Mascarenhas, L.-W. Wang, Similar and dissimilar aspects of III-V semiconductors containing Bi versus N, Phys. Rev. B 71 (2005) 155201, https://doi.org/10.1103/PhysRevB.71.155201.
- [14] A. Duzik, J.C. Thomas, A. van der Ven, J.M. Millunchick, Surface reconstruction stability and configurational disorder on Bi-terminated GaAs(001), Phys. Rev. B 87 (2013) 035313, https://doi.org/10.1103/PhysRevB.87.035313.
- [15] A. Duzik, J.C. Thomas, J.M. Millunchick, J. Lang, M.P.J. Punkkinen, P. Laukkanen, Surface structure of bismuth terminated GaAs surfaces grown with molecular beam epitaxy, Surf. Sci. 606 (2012) 1203–1207, https://doi.org/10.1016/j.susc.2012.03. 021
- [16] A. Beyer, N. Knaub, P. Rosenow, K. Jandieri, P. Ludewig, L. Bannow, S. Koch, R. Tonner, K. Volz, Local Bi ordering in MOVPE grown Ga(As, Bi) investigated by high resolution scanning transmission electron microscopy, Appl. Mater. Today 6 (2017) 22–28, https://doi.org/10.1016/j.apmt.2016.11.007.
- [17] Z. Batool, S. Chatterjee, A. Chernikov, A. Duzik, R. Fritz, C. Gogineni, K. Hild, T.J.C. Hosea, S. Imhof, S.R. Johnson, Z. Jiang, S. Jin, M. Koch, S.W. Koch, K. Kolata, R.B. Lewis, X. Lu, M. Masnadi-Shirazi, J.M. Millunchick, P.M. Mooney, N.A. Riordan, O. Rubel, S.J. Sweeney, J.C. Thomas, A. Thränhardt, T. Tiedje, K. Volz, Bismuth-containing III-V semiconductors: Epitaxial growth and physical properties, Mol. Beam Epitaxy (2013) 139–158, https://doi.org/10.1016/B978-0-12-387839-7.00007-5.
- [18] G. Kresse, J. Hafner, Ab initio molecular dynamics for liquid metals, Phys. Rev. B 47 (1993) 558–561, https://doi.org/10.1103/PhysRevB.47.558.
- [19] G. Kresse, J. Furthmüller, Efficiency of ab-initio total energy calculations for metals and semiconductors using a plane-wave basis set, Comput. Mater. Sci. 6 (1996) 15–50, https://doi.org/10.1016/0927-0256(96)00008-0.
- [20] J.P. Perdew, K. Burke, M. Ernzerhof, Generalized gradient approximation made simple, Phys. Rev. Lett. 77 (1996) 3865–3868, https://doi.org/10.1103/ PhysRevLett. 77.3865.
- [21] S. Grimme, Semiempirical GGA-type density functional constructed with a long-range dispersion correction, J. Comput. Chem. 27 (2006) 1787–1799, https://doi.org/10.1002/jcc.20495.
- [22] G. Kresse, D. Joubert, From ultrasoft pseudopotentials to the projector augmentedwave method, Phys. Rev. B 59 (1999) 1758–1775, https://doi.org/10.1103/ PhysRevB.59.1758.
- [23] H.J. Monkhorst, J.D. Pack, Special points for Brillouin-zone integrations, Phys. Rev. B 13 (1976) 5188–5192, https://doi.org/10.1103/PhysRevB.13.5188.
- [24] J.D. Pack, H.J. Monkhorst, Special points for Brillouin-zone integrations—A reply, Phys. Rev. B 16 (1977) 1748–1749, https://doi.org/10.1103/PhysRevB.16.1748.
- [25] A. Dargys, J. Kundrotas, Handbook on the Physical Properties of Ge, Si, GaAs and InP, Science and Encyclopedia Publishers, 1994.
- [26] P. Deshlahra, E.E. Wolf, W.F. Schneider, A periodic density functional theory analysis of CO chemisorption on Pt(111) in the presence of uniform electric fields, J. Phys. Chem. A 113 (2009) 4125–4133, https://doi.org/10.1021/jp810518x.
- [27] M.K. Rajpalke, W.M. Linhart, M. Birkett, K.M. Yu, J. Alaria, J. Kopaczek, R. Kudrawiec, T.S. Jones, M.J. Ashwin, T.D. Veal, High Bi content GaSbBi alloys, J. Appl. Phys. 116 (2014) 043511, https://doi.org/10.1063/1.4891217.
- [28] R. Alaya, M. Mbarki, A. Rebey, Pressure and composition dependence of structural, electronic and optical properties of GaAsBi alloys, Mater. Sci. Semicond. Process. 40 (2015) 925–930, https://doi.org/10.1016/j.mssp.2015.08.018.
   [29] R.W.G. Wyckoff, Crystal Structures, 2nd ed., Interscience Publishers, New York, NY,
- 1963.
- [30] J. Nyman, G.M. Day, Static and lattice vibrational energy differences between

- polymorphs, CrystEngComm 17 (2015) 5154–5165, https://doi.org/10.1039/
- [31] A.A. Maradudin, G.H. Weiss, E.W. Montroll, Theory of Lattice Dynamics in the Harmonic Approximation, Academic Press, New York, 1963 //catalog.hathitrust.org/Record/001678328.
- [32] S.S. Kapur, M. Prasad, J.C. Crocker, T. Sinno, Role of configurational entropy in the thermodynamics of clusters of point defects in crystalline solids, Phys. Rev. B 72 (2005) 014119, https://doi.org/10.1103/PhysRevB.72.014119.
- [33] J. Puustinen, M. Wu, E. Luna, A. Schramm, P. Laukkanen, M. Laitinen, T. Sajavaara, M. Guina, Variation of lattice constant and cluster formation in GaAsBi, J. Appl. Phys. 114 (2013) 243504, https://doi.org/10.1063/1.4851036.
- [34] R.B. Lewis, M. Masnadi-Shirazi, T. Tiedje, Growth of high Bi concentration

- GaAs1-xBix by molecular beam epitaxy, Appl. Phys. Lett. 101 (2012) 082112, , https://doi.org/10.1063/1.4748172.
- [35] L.C. Bannow, O. Rubel, S.C. Badescu, P. Rosenow, J. Hader, J.V. Moloney, R. Tonner, S.W. Koch, Configuration dependence of band-gap narrowing and localization in dilute GaAs1-xBix alloys, Phys. Rev. B 93 (2016), https://doi.org/10. 1103/PhysRevB.93.205202.
- [36] A. Zunger, S.-H. Wei, L.G. Ferreira, J.E. Bernard, Special quasirandom structures, Phys. Rev. Lett. 65 (1990) 353–356, https://doi.org/10.1103/PhysRevLett. 65.353.
- [37] J. Towns, T. Cockerill, M. Dahan, I. Foster, K. Gaither, A. Grimshaw, V. Hazlewood, S. Lathrop, D. Lifka, G.D. Peterson, R. Roskies, J.R. Scott, N. Wilkins-Diehr, XSEDE: accelerating scientific discovery, Comput. Sci. Eng. 16 (2014) 62–74, https://doi. org/10.1109/MCSE.2014.80.